PHYSICAL REVIEW B, VOLUME 65, 161202(R)

Compressibility and thermal expansion of cubic silicon nitride

J. Z. Jiang,* H. Lindelov, and L. Gerward
Department of Physics, Building 307, Technical University of Denmark, DK-2800 Lyngby, Denmark

K. Ståhl
Department of Chemistry, Building 207, Technical University of Denmark, DK-2800 Lyngby, Denmark

J. M. Recio* and P. Mori-Sanchez
Departamento de Quimica Fisica y Analitica, Facultad de Quimica, Universidad de Oviedo, E-33006 Oviedo, Spain

S. Carlson, M. Mezouar, E. Dooryhee, and A. Fitch
European Synchrotron Radiation Facility (ESRF), Boîte Postal 220, 38000 Grenoble, France

D. J. Frost
Bayerisches Geoinstitut, Universität Bayreuth, D-95440 Bayreuth, Germany

(Received 27 August 2001; revised manuscript received 11 February 2002; published 8 April 2002)

The compressibility and thermal expansion of the cubic silicon nitride (c-Si_3N_4) phase have been investigated by performing *in situ* x-ray powder-diffraction measurements using synchrotron radiation, complemented with computer simulations by means of first-principles calculations. The bulk compressibility of the c-Si_3N_4 phase originates from the average of both Si-N tetrahedral and octahedral compressibilities where the octahedral polyhedra are less compressible than the tetrahedral ones. The origin of the unit cell expansion is revealed to be due to the increase of the octahedral Si-N and N-N bond lengths with temperature, while the lengths for the tetrahedral Si-N and N-N bonds remain almost unchanged in the temperature range 295–1075 K.

DOI: 10.1103/PhysRevB.65.161202 PACS number(s): 65.40.De, 61.10.Eq, 62.20.Fe, 62.50.+p

Recently, after the discovery of a third polymorph of silicon nitride (c-Si_3N_4) synthesized under high-pressure and high-temperature conditions,[1] there has been considerable interest in this field.[2–11] The structure of the material has been determined as a cubic spinel structure at ambient temperature.[1,3–5] It possesses a hardness of about 35.3 GPa,[9] significantly greater than the hardness of the two long-established hexagonal polymorphs: α- and β-Si_3N_4 and slightly harder than that of the stishovite, a high-pressure phase of SiO_2 and hardness of 33 GPa.[12] Besides, the material is stable against oxidation in air up to a temperature of 1673 K.[9] These excellent properties make the c-Si_3N_4 polymorph a promising candidate as an advanced superhard material. The precise knowledge of the compressibility and thermal expansion of the material is of great interest for several practical reasons. Hence, the zero pressure bulk modulus of c-Si_3N_4 has been intensively investigated. However, there is a large scatter of the values reported, 300,[1] 280,[2] 411.9,[6] 308,[8] 284,[8] and 407 GPa (Ref. 10) obtained from theoretical calculations, 300(10) GPa from Hugoniot data[7] and 308(5) GPa from energy-dispersive x-ray powder-diffraction (XRD) measurements.[8] No study of the thermal-expansion behavior of the material has been reported in spite of its relevance in the practical applications of this superhard material. For example, the differences in thermal-expansion coefficients between the substrate and c-Si_3N_4 determine the thermal stress component. In this work, we report the compressibility and thermal-expansion behavior of the c-Si_3N_4 phase by in situ x-ray powder-diffraction measurements using synchrotron radiation, complemented with computer simulations by means of first-principles calculations.

A multianvil octahedra pressure assembly was employed in the synthesis of the cubic spinel Si_3N_4 phase. A mixture of α- and β-Si_3N_4 powders was compressed at 17 ± 0.5 GPa and 2100 K for 1 h. The temperature of the experiment was monitored using a W-3% Re–W-25% Re thermocouple. Further detail for sample preparation is given in Ref. 5. The recovered sample (about 10 mg in weight) was composed of light-yellow transparent sintered crystals with an average grain size of approximately 140 nm determined by optical and scanning electron microscopy and x-ray powder diffraction. Secondary-ion mass spectroscopy measurements on the recovered sample revealed an oxygen impurity less than 1 at. %.

In situ high-temperature (295–1075 K in vacuum) and high-pressure (up to 42 GPa at ambient temperature) x-ray powder-diffraction measurements were performed using synchrotron radiation at beamlines BM16 and ID30, respectively, at ESRF in Grenoble, France. The powder sample, ground from the recovered sample, was placed in an amorphous quartz capillary, pumped down to 10^{-5} mbar and then sealed, and rotated during data collections with a multichannel detector (0.003° accuracy) and a wavelength of 0.71031 Å. A hot air gun was used for high-temperature measurements. The temperature at sample was calibrated using the known temperature dependence of lattice parameter for pure silicon powder in place of the sample position.[13] A diamond-anvil cell with solid Ar as pressure transmitting medium was used for room-temperature compression XRD measurements up to 42 GPa with an image plate mounted on a Fastscan-II detector and a wavelength of 0.3738 Å. The actual pressure was calculated from the wavelength shift of the ruby line

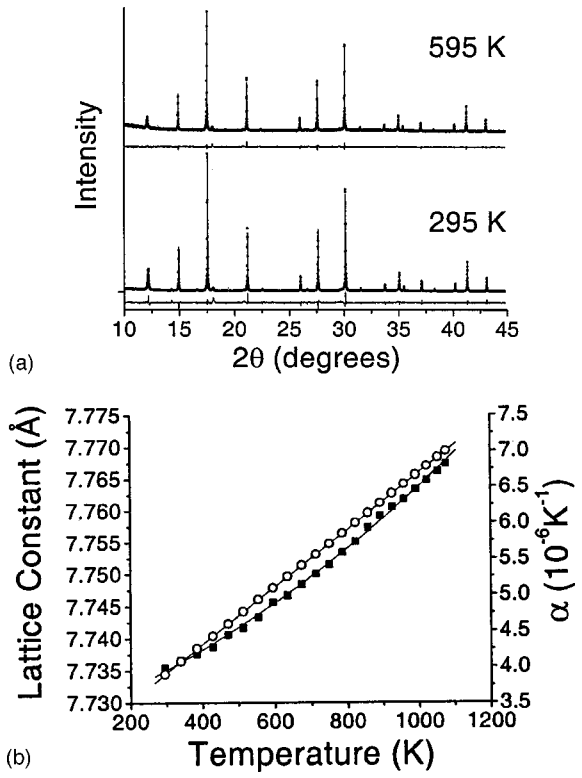

FIG. 1. (a) Rietveld structural refinement profiles of two x-ray powder-diffraction data recorded at 295 and 595 K for the cubic spinel Si_3N_4 phase. (b) The lattice parameter (solid squares) and the linear thermal expansion coefficient (open circles) of the c-Si_3N_4 phase together with fitted curves.

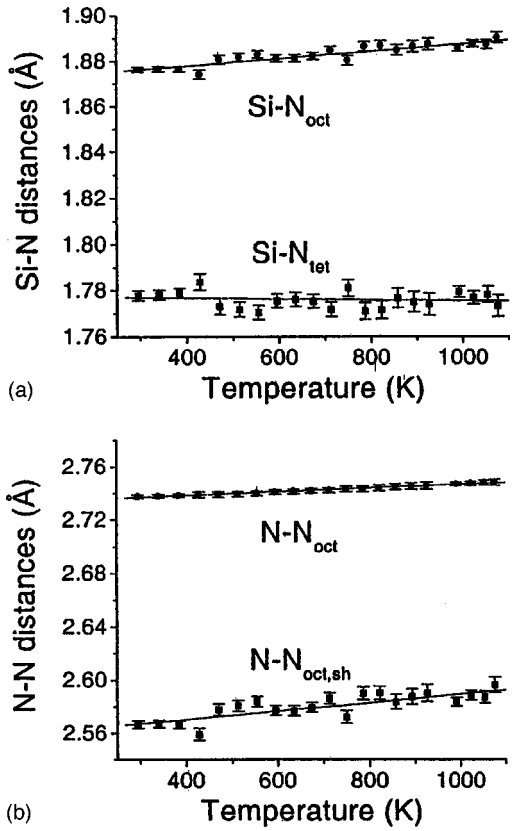

FIG. 2. Temperature dependences of bond lengths for the tetrahedral and octahedral Si-N pairs (a) and N-N pairs (b) obtained from the Rietveld structural refinements for the c-Si_3N_4 phase.

using the nonlinear pressure scale of Mao *et al.*[14] The Rietveld refinement program is a local variation of the LHMP1 program,[17] using the Voigt profile function and Chebyshev polynomial background fitting.

First-principles CRYSTAL calculations[15,16] were performed under the density-functional approximation using the Becke and Perdew-Wang nonlocal exchange and correlation functionals,[17] respectively. Si and N standard Gaussian-type basis sets of triple-ζ quality were adapted to this crystalline structure. The lattice parameter a and the nitrogen internal position (u,u,u) were accurately determined by requiring the total energy of the crystal to be minimum in a set of volume points below and above the experimental equilibrium geometry. Thermal effects on the crystal energy were evaluated through a quasiharmonic nonempirical Debye model that only needs the computed static bulk modulus value as input (details are given in Ref. 18).

High-temperature XRD patterns, recorded in steps of 40 K from 295 to 1075 K for the c-Si_3N_4 phase, are identical except for the thermal expansion. Figure 1(a) exemplifies two Rietveld structure refined XRD patterns recorded at 295 and 595 K. All refinements converged to small residual values. No phase transformation was detected in the temperature range 295–1075 K in vacuum, in agreement with previous data reported for the c-Si_3N_4 sample annealed in air in a temperature range from 295 to 1673 K.[9] The lattice parameter a and the linear thermal-expansion coefficient α of the c-Si_3N_4 phase are shown in Fig. 1(b). The data are fitted with a polynomial function (solid line), $a=7.7274+2.0893\times10^{-5}T+1.5537\times10^{-8}T^2$. Here α is defined as $\alpha=(da/dT)/a$. It is clear that α increases linearly with temperature and can be described with $\alpha=2.716\times10^{-6}\ \mathrm{K}^{-1}+0.004\times10^{-6}T$. The linear thermal-expansion coefficient at 295 K for the c-Si_3N_4 phase is $\alpha=3.89\times10^{-6}\ \mathrm{K}^{-1}$, which is about three times larger than $1.19\times10^{-6}\ \mathrm{K}^{-1}$ at 300 K for β-Si_3N_4 (Refs. 19 and 20) and about four times larger than $1.05\times10^{-6}\ \mathrm{K}^{-1}$ at 300 K for diamond.[21] Our theoretical result $\alpha=3.16\times10^{-6}\ \mathrm{K}^{-1}$ at 300 K supports the experimental data. The calculated lattice parameter and N position at 300 K are, respectively, 7.860 (only 1% larger than the experimental value) and 0.2576 Å (close to 0.2583 from the experiments of Ref. 5). The specific heat capacity at constant volume, $C_v=0.66\ \mathrm{J\,g^{-1}\,K^{-1}}$, Gruneisen parameter $\gamma=1.23$, and Debye temperature $\theta_D=1150$ K, obtained from the simulations at 300 K show also a good agreement with available empirical estimations for this c-Si_3N_4 phase, collected in Ref. 7. Figure 2 depicts the temperature dependences of the bond lengths for the tetrahedral and octahedral sites, obtained from the Rietveld structural refinements. It is clear that the octahedral Si-N bond length increases with temperature, $d=1.871\ \text{Å}+1.610\times10^{-5}T$, while the length for the tetrahedral Si-N bond remains almost unchanged within the experimental uncertainty. Both octahedral N-N bond lengths, shared N-$N_{oct,th}$ $d=2.558\ \text{Å}+3.197\times10^{-5}T$,

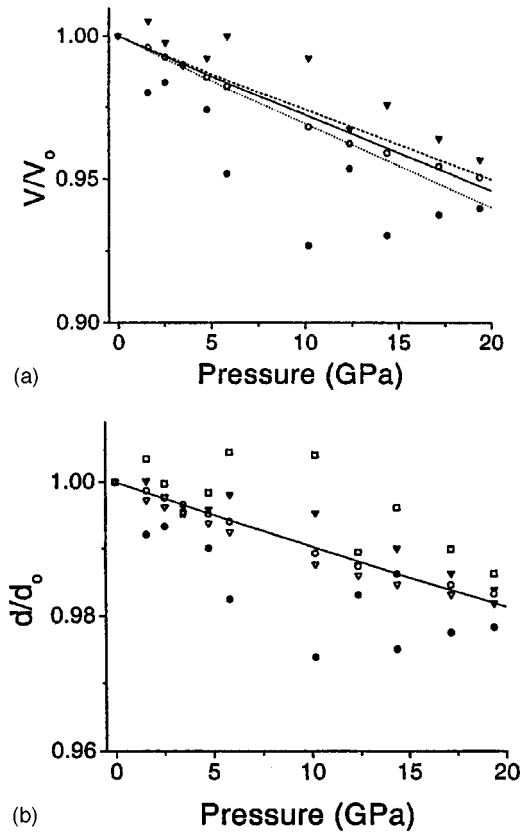

FIG. 3. (a) The reduced unit-cell volume data (open circles), octahedral Si-N polyhedra (solid triangles), and tetrahedral Si-N polyhedra (solid circles), as a function of pressure during compression for the c-Si_3N_4 phase, together with the theoretical results for the reduced unit-cell volume (solid line), for octahedral Si-N polyhedra (dashed line) and for tetrahedral Si-N polyhedra (dotted line). (b) The reduced lattice constant (open circles), octahedral Si-N (solid triangles) and tetrahedral Si-N (solid circles), and both octahedral shared N-$N_{oct,sh}$ (open squares) and unshared N-N_{oct} (open triangles) bond lengths as a function of pressure during compression for the c-Si_3N_4 phase, together with the solid line for the reduced lattice constant obtained from the theoretical calculations.

and unshared N-N_{oct}, $d = 2.733\ \text{Å} + 1.404 \times 10^{-5}$ T, edges of the Si-N octahedral, increase with temperature while the length for the tetrahedral N-N bond [$d_{\text{N-N}_{tet}} d_{\text{Si-N}_{tet}} = 1.633$, not shown in Fig. 2(b)] remains almost unchanged. The octahedral Si-N bond angle varies randomly around 86.35° $\pm 0.06°$ in the whole temperature range while the tetrahedral Si-N bond angle is constant of 109.47 due to the symmetry. The strong temperature dependence of the octahedral Si-N and N-N bonds causes a large linear thermal-expansion coefficient at 295 K for the c-Si_3N_4 phase as compared to β-Si_3N_4 because in β-Si_3N_4 only tetrahedral bonds exist. This picture is consistent with the results observed in Ref. 19, i.e., the thermal expansion for tetrahedral bonds is smaller than that for octahedral bonds.

A large number of XRD patterns were recorded at pressures ranging from 0 to approximately 42 GPa at ambient temperature. Up to a pressure of 42 GPa, no phase transformation was observed. At pressures above 20 GPa, Bragg peaks become broadened and strain deduced from Rietveld structural refinements starts to increase with pressure. The results infer that a transition from a hydrostatic state below 20 GPa into a nonhydrostatic one above 20 GPa occurs for the sample in the diamond-anvil cell. Hence, pressure-volume data below 20 GPa will be further used to explore the compression behavior of the c-Si_3N_4 phase. Figure 3 shows the reduced unit-cell volume data, octahedral Si-N polyhedra, $V_{oct} = 128V(u - \frac{3}{8})^2 u/3$, and tetrahedral Si-N polyhedra, $V_{tet} = 64V(u - 1/8)^3/3$ [Fig. 3(a)], where V is the unit-cell volume. Also shown are the reduced lattice constant, octahedral and tetrahedral Si-N bond lengths, and both octahedral shared N-$N_{oct/sh}$ and unshared N-N_{oct} bond lengths as a function of pressure during compression [Fig. 3(b)]. The octahedral Si-N bond angle varies randomly around $86.58° \pm 0.15°$ in the whole pressure range while the tetrahedral Si-N bond angle is constant of 109.47 due to the symmetry. The bulk modulus at zero pressure, B_0, and the first pressure derivative, B_0', for the c-Si_3N_4 phase at ambient temperature are found to be 317 ± 11 GPa and 2.3 ± 2.1 or 309 ± 3 GPa and 4.0 (constrained), respectively, using the Birch equation of state.[22] These and other data are listed in Table I. The experimental values of B_0 and B_0', obtained here are in good agreement with data reported in Refs. 1, 2, 7, 8. We found that the Si-N octahedral polyhedra are slightly less compressible than the Si-N tetrahedral ones, although there is some scatter in the experimental data due to a large uncertainty of the parameter u estimated from the Rietveld structural refinements. The bulk modulus of the c-Si_3N_4 phase can be estimated as the average of both tetrahedral and octahedral moduli, which are controlled by the Si-N pair, as illustrated by the linear curve in Fig. 3(b). The computed pressure diagrams for reduced volumes [Fig. 3(a)] and bond lengths [Fig. 3(b)] are consistent with the experimental points. Besides, the theoretical results predict the same compressibility sequence obtained in the XRD measurements for polyhedra and distances. In Table I, we include computed

TABLE I. Collected values of the bulk modulus at zero pressure, B_0, and the first pressure derivative, B_0', for the c-Si_3N_4 phase. The lower part of the table contains the results obtained in this work.

B_0 (GPa)	B_0'	Comments
300		Theoretical (Ref. 1)
280	3.48	Theoretical (Ref. 2)
411.9		Theoretical (Ref. 6)
308	3.9	Theoretical (Ref. 8)
284	3.9	Theoretical (Ref. 8)
305		Theoretical (Ref. 8)
407	3.33	Theoretical (Ref. 10)
300 ± 10	3.0 ± 0.1	Experimental (Ref. 7)
308 ± 5	4.0 ± 0.2	Experimental (Ref. 8)
328	2.8	Theoretical (bulk)
361	2.9	Theoretical (Si-N octahedra)
298	2.6	Theoretical (Si-N tetrahedra)
309 ± 3	4.0 fixed	Experimental
317 ± 11	2.3 ± 2.1	Experimental

polyhedral and bulk equation of state parameters at 300 K. Our calculations yield B_0 for the bulk only slightly overestimated with respect to the present experimental value. The lower compressibility of the octahedra is quantified with a splitting between octahedral and tetrahedral B_0 values of 63 GPa. Note also that the average of the octahedral and tetrahedral B_0 values reproduces the value for the bulk. This result has been explained as a consequence of the low dependence of the parameter u on pressure.[23]

One striking feature revealed from Figs. 2 and 3 is that the octahedral Si-N and N-N bond lengths are less compressible than the tetrahedral ones while for thermal expansion, the octahedral Si-N and N-N bond lengths are more expanding than the tetrahedral ones. The results indicate a different bond strength versus bond-length behavior for the octahedral and tetrahedral sites in the c-Si_3N_4 phase. During compression, bond strength increases faster for the octahedral sites than the tetrahedral ones, with the result that the octahedral polyhedra are less compressible than the tetrahedral ones, as detected in Fig. 3. On the other hand, during thermal expansion the bond strength for the octahedral sites may increase more slowly than the tetrahedral ones. Consequently, the bond length for the octahedral site increases faster with temperature than the tetrahedral one, as observed experimentally in Fig. 2. The experimental results described here have already triggered further theoretical work on this matter.

*Corresponding author,: Department of Physics, Building 307, Technical University of Denmark, DK-2800 Lyngby, Denmark. FAX: +45 45 93 23 99. Email address: jiang@fysik.dtu.dk

[1] A. Zerr *et al.*, Nature (London) **400**, 340 (1999).
[2] S. D. Mo *et al.*, Phys. Rev. Lett. **83**, 5046 (1999); W. Y. Ching *et al.*, Phys. Rev. B **61**, 8696 (2000).
[3] T. Sekine *et al.*, Appl. Phys. Lett. **76**, 3706 (2000).
[4] M. Schwarz *et al.*, Adv. Mater. **12**, 883 (2000).
[5] J. Z. Jiang *et al.*, Europhys. Lett. **51**, 62 (2000).
[6] C. M. Marian, M. Castreich, and J. D. Gale, Phys. Rev. B **62**, 3117 (2000).
[7] H. He *et al.*, Phys. Rev. B **62**, 11 412 (2000).
[8] E. Soignard *et al.*, J. Phys.: Condens. Matter **13**, 557 (2001).
[9] J. Z. Jiang *et al.*, J. Phys.: Condens. Matter **13**, L515 (2001).
[10] P. Mori-Sanchez *et al.*, Europhys. Lett. **54**, 760 (2001).
[11] T. Sekine *et al.*, Appl. Phys. Lett. **78**, 3050 (2001); I. Tanaka *et al.*, *ibid.* **78**, 2134 (2001).
[12] J. M. Leger *et al.*, Nature (London) **383**, 401 (1996).
[13] Y. Okada and Y. Tokumaru, J. Appl. Phys. **56**, 314 (1984).
[14] H. K. Mao *et al.*, J. Appl. Phys. **49**, 3276 (1978).
[15] J. Z. Jiang *et al.*, Phys. Rev. B **55**, 14 830 (1997).
[16] V. R. Saunders *et al.*, CRYSTAL98 User's Manual (University of Torino, Torino, 1998).
[17] A. D. Becke, Phys. Rev. A **38**, 3098 (1988); J. P. Perdew, in *Electronic Structure of Solids*, edited by P. Ziesche and H. Eschrig (Academic, Berlin, 1991).
[18] E. Francisco *et al.*, J. Phys. Chem. A **102**, 1595 (1998).
[19] I. C. Huseby, G. A. Slack, and R. H. Arendt, Bull. Am. Ceram. Soc. **60**, 919 (1981).
[20] R. J. Bruls, H. T. Hintzen, G. de With, R. Metselaar, and J. C. van Miltenburg, J. Phys. Chem. Solids **62**, 783 (2001).
[21] G. A. Slack and S. F. Bartram, J. Appl. Phys. **46**, 89 (1975).
[22] F. Birch, J. Appl. Phys. **9**, 279 (1938); Phys. Rev. **71**, 809 (1947).
[23] J. M. Recio *et al.*, Phys. Rev. B **63**, 184101 (2001).